



1 **Ocean liming effects on dissolved organic matter dynamics**

2

3 Chiara Santinelli<sup>1</sup>, Silvia Valsecchi<sup>1,2,3</sup>, Simona Retelletti Brogi<sup>1,4</sup>, Giancarlo Bachi<sup>1</sup>, Giovanni  
4 Checcucci<sup>1</sup>, Mirco Guerrazzi<sup>1</sup>, Elisa Camatti<sup>5</sup>, Stefano Caserini<sup>3,6</sup>, Arianna Azzellino<sup>2,3</sup>, Daniela  
5 Basso<sup>3,7</sup>

6

7 <sup>1</sup> Consiglio Nazionale delle Ricerche (CNR), Istituto di Biofisica. Via Moruzzi 1, 56124 Pisa (PI), Italia.

8

9 <sup>2</sup> Politecnico di Milano, Dipartimento di Ingegneria Civile ed Ambientale. Piazza Leonardo da Vinci 32, 20133 Milano (MI), Italia.

9

10 <sup>3</sup> Consorzio Nazionale Interuniversitario per le Scienze del Mare (CoNISMa). Piazzale Flaminio 9, 00196 Roma (RM), Italia.

10

11 <sup>4</sup> Istituto di Oceanografia e Geofisica Sperimentale (OGS), Sezione di Oceanografia. Via Piccard 54, 34151 Trieste (TS), Italia.

11

12 <sup>5</sup> Consiglio Nazionale delle Ricerche (CNR), Istituto di Scienze Marine. Arsenale Tesa 104, Castello 2737/F - 30122 Venezia (VE), Italia.

12

13 <sup>6</sup> Università di Parma, Dipartimento di Ingegneria e Architettura. Parco Area delle Scienze 181/A, 43124 Parma (Pr), Italia.

13

14 <sup>7</sup> Università degli Studi di Milano-Bicocca, Dipartimento di Scienze dell'ambiente e della terra. Piazza della Scienza 4, 20126 Milano (MI), Italia.

14

15

16

*Correspondence to:* Chiara Santinelli (chiara.santinelli@ibf.cnr.it)

17



18 **Abstract.** Ocean liming has gained attention as a potential solution to mitigate climate change by actively removing  
19 carbon dioxide (CO<sub>2</sub>) from the atmosphere. The addition of hydrated lime (Ca(OH)<sub>2</sub>) into oceanic surface water leads to  
20 an increase in alkalinity, which in turn promotes the uptake and sequestration of atmospheric CO<sub>2</sub>.  
21 Despite the potential of this technique, its effects on the marine ecosystem are still far to be understood, and there is  
22 currently no information on the potential impacts on the concentration and quality of Dissolved Organic Matter (DOM),  
23 that is the largest, the most complex and yet the least understood mixture of organic molecules on Earth. The aim of this  
24 study is to provide the first experimental evidence about the potential effects of pH peaks, that might be generated by the  
25 Ca(OH)<sub>2</sub> dissolution in seawater, on DOM dynamics by assessing changes in its concentration and optical properties  
26 (absorption and fluorescence).  
27 To investigate the effects of liming on DOM pools with different concentrations and quality, seawater was collected from  
28 two contrasting environments: the oligotrophic Mediterranean Sea (MedSea), known for its Dissolved Organic Carbon  
29 (DOC) concentration comparable to that observed in the oceans, and the eutrophic Baltic Sea (BalSea), characterized by  
30 high DOM concentration mostly of terrestrial origin. Ca(OH)<sub>2</sub> was added in both waters, to reach a pH of 9 and 10.  
31 Our findings reveal that the addition of hydrated lime has a noticeable effect on DOM dynamics in both the MedSea and  
32 BalSea, determining a reduction in DOC concentration and a change in the optical properties (absorption and  
33 fluorescence) of DOM. These effects, detectable at pH 9, become significant at pH 10 and are more pronounced in the  
34 MedSea than in the BalSea. These potential short-term effects should be considered within the context of the physico-  
35 chemical properties of seawater and the seasonal variability.



## 36 1 Introduction

37 Oceans are a natural sink for atmospheric CO<sub>2</sub> having the potential to mitigate its increase and therefore the effects of  
38 climate change (Gattuso et al., 2013; Heinze et al., 2015). The massive amount of atmospheric CO<sub>2</sub> absorbed by the  
39 oceans in the last decades (~ 30-40% of anthropogenic emissions), is generating dramatic global-scale changes in seawater  
40 chemistry, such as a decrease in pH, in carbonate concentration and in the ocean buffering capacity (Chikamoto et al.,  
41 2023). Even if the ongoing efforts toward a global reduction of anthropogenic CO<sub>2</sub> emissions should be rapidly intensified,  
42 the available projections highlight the need for additional strategies, such as the development of efficient ocean-based  
43 Negative Emission Technologies (NETs) (Royal Society and Royal Academy of Engineering, 2018; Calvin et al., 2023).  
44 Some NETs are not only capable of removing atmospheric CO<sub>2</sub> and store it as bicarbonate ions into the oceans, but also  
45 of increasing the water pH, restoring ocean buffering capacity to the pre-industrial era (Gore et al., 2019; Butenschön et  
46 al., 2021). One of these NETs is Ocean Alkalinity Enhancement (OAE) (also called Artificial Ocean Alkalinization,  
47 AOA), which relies on the dissolution of alkaline minerals such as hydrated lime (calcium hydroxide, Ca(OH)<sub>2</sub>) into the  
48 oceans (Kheshgi, 1995). Although the exact amount of hydrated lime to be released, as well as its sparging methods, is  
49 still under debate one of the proposals is to discharge highly concentrated slurry (*lime milk*) from large cargo ships, tankers  
50 and/or dedicated vessels. Modeling studies, simulating the flow dynamics in the wake of a sparging ship (Caserini et al.,  
51 2021), indicate that the addition of Ca(OH)<sub>2</sub> with an initial particle radius of 45 μm into seawater can cause a temporary,  
52 sharp increase in pH of about 1 unit, becoming lower than 0.2 units, 1400 – 1600 m far from the discharge site (in the  
53 hypothesis of a discharge rate of 10 kg s<sup>-1</sup>, Caserini et al., 2021).

54 The discharge of alkaline minerals may trigger the inorganic precipitation of calcium carbonate (CaCO<sub>3</sub>), reducing the  
55 efficiency of the CO<sub>2</sub> sink and negatively affecting seawater transparency and photosynthetic rates (González and Ilyina,  
56 2016), with possible consequences for the biogeochemical cycles and the functioning of the marine ecosystem (Camatti  
57 et al., 2024). The side effects of OAE techniques on the marine environment need to be thoroughly investigated before  
58 making any decision on their use. To the best of our knowledge, there is no information on the effects that ocean liming  
59 may have on Dissolved Organic Matter (DOM) and its chromophoric fraction (CDOM, i.e. the light-absorbing fraction).  
60 Holding an amount of carbon of 660 billion metric tons and being the most concentrated dissolved component in the  
61 oceans (Hansell et al., 2009), every action that could modify seawater chemistry is expected to have an impact on this  
62 key component of the carbon cycle. DOM represents the main source of energy for heterotrophic prokaryotes, a change  
63 in its concentration and/or quality could therefore have a cascading effect on the functioning of marine ecosystem.

64 The aim of this study is to provide the first experimental evidence about the potential effects of hydrated lime addition on  
65 DOM dynamics in the oceans, by assessing changes in its concentration and optical properties (absorption and  
66 fluorescence). In order to investigate the impact on DOM pool with different origin and optical properties, seawater was  
67 collected from two highly diverse environments; (1) the oligotrophic Mediterranean Sea (MedSea), characterized by  
68 Dissolved Organic Carbon (DOC) concentration comparable to those observed in the open oceans, and (2) the eutrophic  
69 Baltic Sea (BalSea), characterized by high DOC concentration, mostly of terrestrial origin.

70

## 71 2 Materials and methods

72 In order to investigate the effects of ocean liming on DOM dynamics, an ultra-pure Ca(OH)<sub>2</sub> powder was added to natural  
73 seawater and changes in DOC concentration, absorption and fluorescence of CDOM were followed for 24 hours at the  
74 laboratories of the Biophysics Institute, CNR (Pisa, Italy). The experiments were carried out at pH 9 and 10, based on the



75 results of Caserini et al. (2021), which assumes conservative values of lime milk ( $\text{Ca}(\text{OH})_2$  86.5 g/l) discharge rates ( $\leq 25$   
 76 kg/s) in the ships' wake.  $\text{Ca}(\text{OH})_2$  was provided by UNICALCE (Sedrina (BG), Italy) and supplied as powder (Tab. S1).  
 77 Seawater was collected at Marina di Pisa, Tyrrhenian Sea, Italy (MedSea) and in the coastal area surrounding Riga, Latvia  
 78 (BalSea) (Tab. 1).

79

	Sampling Date	Salinity	pH	DOC ( $\mu\text{M}$ )	$a_{254}$ ( $\text{m}^{-1}$ )	$S_{275-295}$ ( $\text{nm}^{-1}$ )
MedSea	Mar-22	38	8.2	$66 \pm 0.5$	1.9	0.024
BalSea	Apr-22	6	8.1	$364 \pm 3$	24.5	0.021

80 **Table 1: Chemical and physical properties of the MedSea and BalSea water used for the experiment.**

81

## 82 2.1 Experimental setup

83 In order to investigate the impact of slaked lime on chemical-physical processes affecting DOM dynamics, seawater was  
 84 sterilized by filtration through a 0.2  $\mu\text{m}$  pore size filter (Polycap AS36 filter capsule, Whatman, UK) using a peristaltic  
 85 pump (Masterflex™ L/S™, Germany). Salinity was measured by using a HI 9033portable probe (Hanna Instruments,  
 86 USA). The experiments were carried out in 2 L acid-washed polycarbonate®Nalgene bottles as follows:

87

### 1. MedSea

88

a. Treatment: filtered surface seawater enriched with  $\text{Ca}(\text{OH})_2$  powder to reach:

89

- pH 9, [ $\text{Ca}(\text{OH})_2$ ] 0.04 g/L

90

- pH 10, [ $\text{Ca}(\text{OH})_2$ ] 0.25 g/L

91

b. Control: filtered surface seawater (pH = 8.2)

92

### 2. BalSea

93

a. Treatment: filtered surface seawater enriched with  $\text{Ca}(\text{OH})_2$  powder to reach

94

- pH of 9, [ $\text{Ca}(\text{OH})_2$ ] 0.01 g/L

95

- pH 10, [ $\text{Ca}(\text{OH})_2$ ] 0.06 g/L

96

b. Control: filtered surface seawater (pH = 8.1)

97

All the experiments were carried out in triplicates and the bottles were stored in the dark and at room temperature ( $22 \pm$

98

1 °C). Immediately after the addition of the  $\text{Ca}(\text{OH})_2$  powder, the bottles were gently mixed. Before and after powder

99

addition and before each sampling time, pH was measured using an edge HI2002-02 pH-meter (Hanna Instruments, USA).

100

Subsamples for DOC (40 mL) and CDOM/FDOM (60 mL) analyses were collected before  $\text{Ca}(\text{OH})_2$  addition and 5', 30',

101

3 h and 22 h after  $\text{Ca}(\text{OH})_2$  addition.

102

The bottles were gently mixed before subsampling. Since carbonate sedimentation was clearly visible at the bottom of

103

the bottles after 22 hours, an additional sample of the supernatant was collected before mixing.

104

Samples for CDOM/FDOM analyses were brought to  $\text{pH } 7.5 \pm 1.0$  with high purity 2 M HCl, to avoid the effect of pH

105

on DOM absorption and fluorescence and filtered through a PES 0.2  $\mu\text{m}$  pore size syringe filter (Minisart 16534K,

106

Sartorius, Germany), to avoid the scattering due to the presence of carbonate particles in solution.



107

## 108 **2.2 DOC**

109 Samples for DOC analysis were acidified at pH 2 with high purity 2 M HCl. DOC measurements were carried out with a  
110 TOC-L analyzer (Shimadzu, Japan), by high temperature catalytic oxidation following Santinelli et al. (2015). Samples  
111 were sparged for 3 min with CO<sub>2</sub>-free ultrahigh purity nitrogen to remove inorganic carbon. 150 µL of the sample were  
112 injected into the furnace after a three-fold rinsing with the sample to be analyzed. From 3 to 5 replicate injections were  
113 performed until the analytical error was lower than 1%. A four-point calibration curve was measured using a standard  
114 solution of potassium hydrogen phthalate in the same concentration range as the samples. The system blank was measured  
115 every day at the beginning and the end of the analyses using low-carbon water (2-3 µM C). The instrument performance  
116 was verified daily using the DOC Consensus Reference Material (CRM) (Hansell, 2005) (CRM Batch #20/08-20, nominal  
117 concentration of 42 ± 1 µM; measured concentration 40 ± 2 µM, n of samples = 76).

118

## 119 **2.3 CDOM optical properties**

### 120 **2.3.1 Absorption**

121 Absorption spectra were measured between 230 and 700 nm with a UV-Vis spectrophotometer (Mod-7850, Jasco, USA),  
122 using a 10 cm quartz cuvette. The absorption spectrum of Milli-Q water was subtracted from each sample spectrum. The  
123 absorption coefficient at 254 nm ( $a_{254}$ ) and the spectral slope between 275 and 295 nm ( $S_{275-295}$ ) were calculated from the  
124 absorption spectra using the ASFit tool (Omanović et al., 2019).  $a_{254}$  is used to have semi-quantitative information on  
125 CDOM, since primary CDOM absorption is caused by conjugated systems having the absorption peak near 254 nm  
126 (Weishaar et al., 2003; Del Vecchio and Blough, 2004).  $S_{275-295}$  can be related to changes in the average aromaticity and  
127 molecular weight of the molecules in the CDOM pool (Helms et al., 2008).

128

### 129 **2.3.2 Fluorescence**

130 Fluorescence excitation-emission matrices (EEMs) were recorded with an Aqualog fluorometer (Horiba-Jobin Yvon,  
131 UK), using a 1 cm quartz cuvette. Excitation ranged between 250 and 450 nm at 5 nm increments; emission was recorded  
132 between 212 and 619 nm at 3 nm increments. The EEMs were elaborated using the TreatEEM software (Omanović et al.,  
133 2023). EEMs were corrected for instrumental bias in excitation and emission, and Rayleigh and Raman scatter peaks were  
134 removed using the monotone cubic interpolation (shape-preserving). EEMs were normalized to the water Raman signal,  
135 dividing the fluorescence by the integrated Raman band of Milli-Q water ( $\lambda_{ex} = 350$  nm,  $\lambda_{em} = 371-428$  nm; Lawaetz and  
136 Stedmon, 2009) measured on the same day of the analyses. The fluorescence intensity is therefore reported as equivalent  
137 to water Raman Units (R.U.).

138 Parallel factor analysis (PARAFAC) was separately applied to the MedSea (number of EEMs: 63) and BalSea (number  
139 of EEMs: 50) samples, using the decomposition routines of the EEMs toolbox for MATLAB software (drEEM) (Murphy  
140 et al., 2013). The PARAFAC validated a 3-component model for both the MedSea and the BalSea (Fig. S1 and S2).



141 OpenFluor, an online database of environmental fluorescence spectra, was used as a validation tool to characterize the  
142 three components (Tab. S2 and S3). OpenFluor compares excitation and emission spectra of the validated components  
143 with all the components present in the database and allows comparing the spectra using the Tucker Congruence  
144 Coefficient (TCC; Murphy et al. (2014)).

145

## 146 2.4 Statistical analyses

147 For all parameters, differences were tested using the Kruskal–Wallis nonparametric test and were considered significant  
148 at the threshold of  $p < 0.05$ . All statistical analyses were performed using OriginPro version 9 (OriginLab, USA).

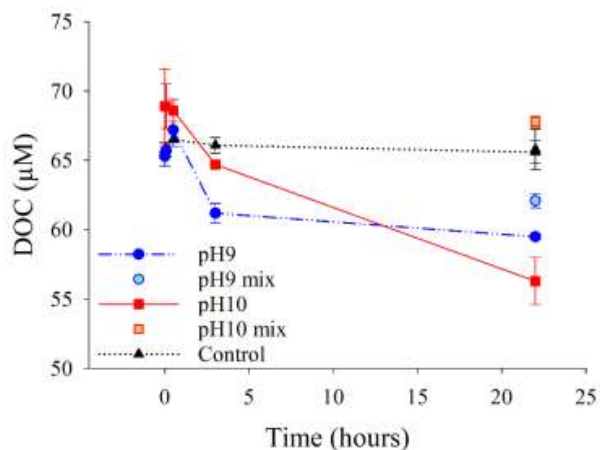
149

## 150 3. Results

### 151 3.1 Mediterranean Sea

#### 152 3.1.1 DOC

153 In the MedSea, DOC concentration was  $67 \pm 2 \mu\text{M}$ . Three hours after  $\text{Ca}(\text{OH})_2$  addition, a  $4 \mu\text{M}$  (6%) DOC decrease was  
154 observed in both treatments (Fig. 1). A further decrease was observed in the supernatant of the unmixed sample 22 h after  
155 the addition, with DOC reaching  $59 \pm 0.2 \mu\text{M}$  (12% decrease) at pH 9 and  $56 \pm 1 \mu\text{M}$  (16% decrease) at pH 10. It is  
156 noteworthy that such a decline was only observed in the unmixed samples, whereas no significant change was observed  
157 in the mixed samples 22 h after the addition (Fig.1).



158

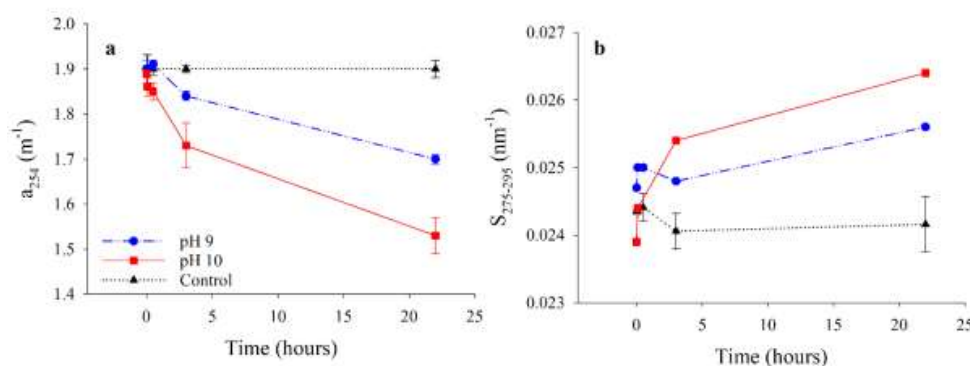
159 **Figure 1: Trend of DOC concentration in the MedSea treatments at pH 9 and 10, and in the control. Error bars**  
160 **refer to the standard deviation among the 3 replicates.**

161



### 162 3.1.2 CDOM Absorption

163 A slight decrease in  $a_{254}$  was observed 3 hours after  $\text{Ca}(\text{OH})_2$  addition at both pH (9 and 10). Interestingly, 22 h after the  
 164 addition, in the supernatant of unmixed bottles, a marked decrease of  $0.2 \text{ m}^{-1}$  (11%) and  $0.4 \text{ m}^{-1}$  (20%) was observed (Fig.  
 165 2a) together with an increase in  $S_{275-295}$  from  $0.0241 \text{ nm}^{-1}$  to  $0.0256 \text{ nm}^{-1}$  (6%) and to  $0.0264 \text{ nm}^{-1}$  (10%) at pH 9 and 10,  
 166 respectively (Fig. 2b). Mixed samples were not collected, since scattering due to the particles would have affected the  
 167 results.



168

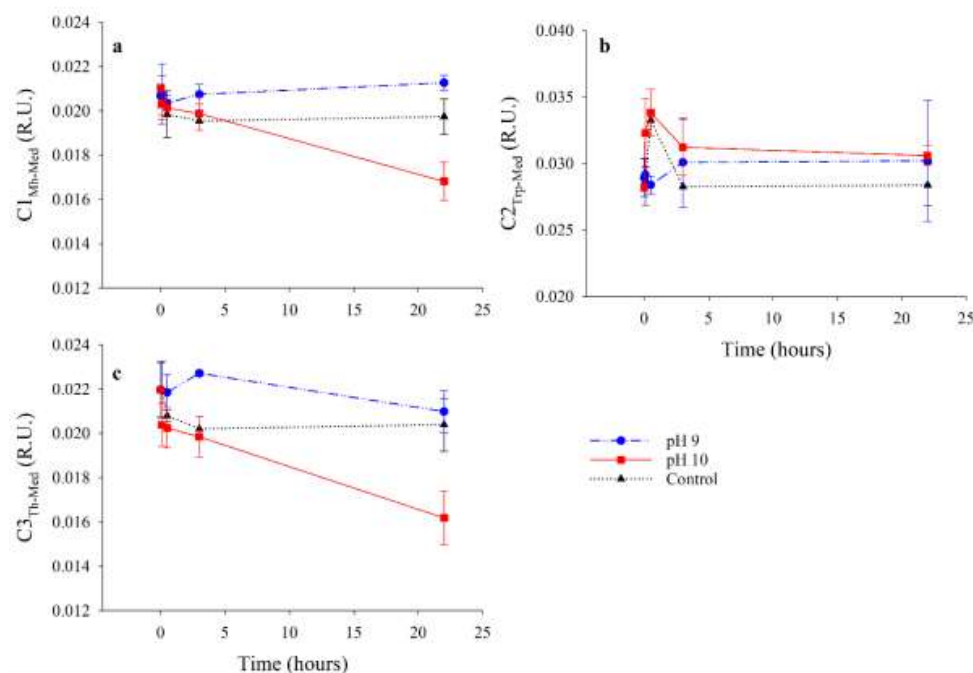
169 **Figure 2: Trend of  $a_{254}$  (a) and  $S_{275-295}$  (b) in the MedSea treatments at pH 9 and 10, and in the control. Error**  
 170 **bars refer to the standard deviation among the 3 replicates.**

171

### 172 3.1.3 FDOM fluorescence

173 The PARAFAC validated a 3 component model for the MedSea EEMs (Fig. S1, Tab. S2). Component 1 ( $\lambda_{\text{Ex}}/\lambda_{\text{Em}}$ : 315/409  
 174 nm, Fig. S1a) shows spectroscopic characteristics similar to Coble's peak M ( $\lambda_{\text{Ex}}/\lambda_{\text{Em}}$ : 312/[380]420; Coble (1996)). The  
 175 comparison with similar components in the OpenFluor database (matches with a TCC > 0.95) allowed to characterize it  
 176 as marine humic-like ( $\text{C1}_{\text{Mh-Med}}$ ). Component 2 ( $\lambda_{\text{Ex}}/\lambda_{\text{Em}}$ : 275/331 nm, Fig. S1b) shows spectroscopic characteristics  
 177 similar to Coble's peak T ( $\lambda_{\text{Ex}}/\lambda_{\text{Em}}$ : 275/340 nm; Coble (1996)). The comparison with similar components in the  
 178 OpenFluor database (matches with a TCC > 0.95) allowed to characterize it as Tryptophan-like ( $\text{C2}_{\text{Tp-Med}}$ ). Component  
 179 3 ( $\lambda_{\text{Ex}}/\lambda_{\text{Em}}$ : 260/[380]456 nm, Fig. S1c) shows spectroscopic characteristics similar to Coble's peaks C and A ( $\lambda_{\text{Ex}}/\lambda_{\text{Em}}$ :  
 180 350/451 and 245/451 nm, respectively; Coble (1996)). The comparison with similar components in the OpenFluor  
 181 database (matches with a TCC > 0.95) allowed to characterize it as terrestrial humic-like ( $\text{C3}_{\text{Th-Med}}$ ).

182  $\text{C1}_{\text{Mh-Med}}$  did not show significant changes over the incubation time at pH 9 and in the control (Fig. 3a). At pH 10, a  
 183 decrease of 0.004 R.U. (19%) was observed 22 h after the addition.  $\text{C2}_{\text{Tp-Med}}$  did not show significant changes during the  
 184 incubation, neither in the treatments nor in the control (Fig. 3b).  $\text{C3}_{\text{Th-Med}}$  showed variations only at pH 10 (Fig. 3c), with  
 185 a slight decrease 3 hours after the addition, and a significant decrease of 0.006 R.U. (26%) at the end of the incubation  
 186 (22 h).



187

188 **Figure 3: Trend of the fluorescent intensity of  $C1_{Mh-Med}$  (a),  $C2_{Trp-Med}$  (b) and  $C3_{Th-Med}$  (c) in the MedSea**  
189 **treatments at pH 9 and 10, and in the control. Error bars refer to the standard deviation among the 3 replicates.**

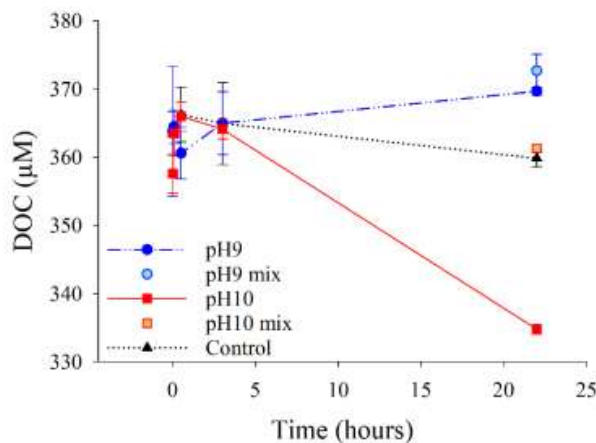
190

### 191 3.2 Baltic Sea (BalSea)

#### 192 3.2.1 DOC

193 In the BalSea, DOC concentration was  $362 \pm 3 \mu\text{M}$ . No significant change was observed 3 hours after  $\text{Ca}(\text{OH})_2$  addition  
194 in both treatments (pH 9 and 10) (Fig. 4). At the end of the experiment (22 h), DOC decreased by  $27 \mu\text{M}$  (7 %) at pH 10,  
195 whereas no significant change was observed at pH 9. It is noteworthy that DOC showed significant differences between  
196 the mixed and unmixed samples at pH 10, whereas in the mixed samples DOC was similar to the control (Fig. 4).





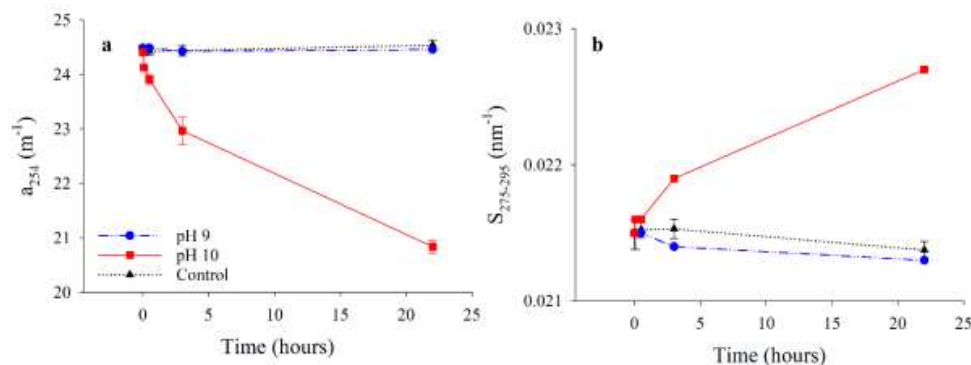
197

198 **Figure 4: Trend of DOC concentration in the BalSea treatments at pH 9 and 10 and in the control. Error bars**  
 199 **refer to the standard deviation among the 3 replicates.**

200

### 201 3.2.2 CDOM

202 Twenty-two hours after the addition of  $\text{Ca}(\text{OH})_2$ ,  $a_{254}$  decreased by  $0.03 \text{ m}^{-1}$  (0.3%), and  $3.7 \text{ m}^{-1}$  (15%) at pH 9 and pH  
 203 10, respectively (Fig. 5a).  $S_{275-295}$  increased from  $0.0215 \text{ nm}^{-1}$  to  $0.023 \text{ nm}^{-1}$  (6%) at pH 10, whereas no significant change  
 204 was observed at pH 9 (Fig. 5b). The change in CDOM is therefore visible only at pH 10 (Fig. 5)



205

206 **Figure 5: Trend of  $a_{254}$  (a) and  $S_{275-295}$  (b) in the BalSea treatments at pH 9 and 10, and in the control. Error bars**  
 207 **refer to the standard deviation among the 3 replicates.**

208

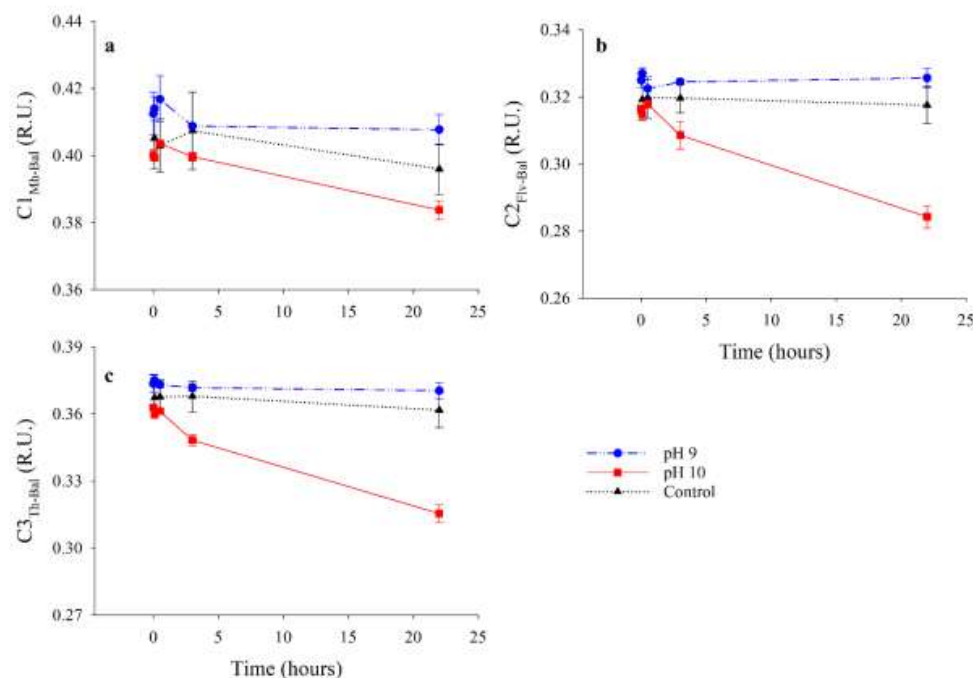


209 **3.2.3 FDOM**

210 The PARAFAC validated a 3-component model for the BalSea EEMs experiment (Fig. S2, Tab. S3). Component 1  
 211 ( $\lambda_{Ex}/\lambda_{Em}$ : 290/400 nm, Fig. S2) shows spectroscopic characteristics similar to Coble’s peak M ( $\lambda_{Ex}/\lambda_{Em}$ : 312/[380]420;  
 212 Coble (1996)). The comparison with similar components in the OpenFluor database (matches with a TCC > 0.95) allowed  
 213 to characterize it as marine humic-like ( $C1_{Mh-Bal}$ ). Component 2 ( $\lambda_{Ex}/\lambda_{Em}$ : 330/452 nm, Fig. S2) shows spectroscopic  
 214 characteristics similar to Coble’s peak C ( $\lambda_{Ex}/\lambda_{Em}$ : 350/451; Coble (1996)). The comparison with similar components in  
 215 the OpenFluor database (matches with a TCC > 0.95) allowed to characterize it as Fulvic-like ( $C2_{Fiv-Bal}$ ). Component 3  
 216 ( $\lambda_{Ex}/\lambda_{Em}$ : 280/485 nm, Fig. S2) shows spectroscopic characteristics similar to Coble’s peak A ( $\lambda_{Ex}/\lambda_{Em}$ : 260/[380]460 nm;  
 217 Coble (1996)). The comparison with similar components in the OpenFluor database (matches with a TCC > 0.95) allowed  
 218 to characterize it as Terrestrial humic-like ( $C3_{Th-Bal}$ ).

219  $C1_{Mh-Bal}$  did not show significant changes during the incubation neither in the treatments nor in the control (Fig. 6a).  $C2_{Fiv-}$   
 220  $Bal$  did not show significant changes during the incubation at pH 9 and in the control, whereas a decrease of 0.03 R.U.  
 221 (9%) was observed at pH 10 between 30 minutes and 22 hours (Fig. 6b).  $C3_{Th-Bal}$  did not show significant changes during  
 222 the incubation at pH 9 and in the control, whereas a decrease of 0.04 R.U. (11%) was observed at pH 10 between 30  
 223 minutes and 22 hours (Fig. 6c).

224



225

226 **Figure 6: Trend of the fluorescent intensity of  $C1_{Mh-Bal}$  (a),  $C2_{Fiv-Bal}$  (b) and  $C3_{Th-Bal}$  (c) in the BalSea treatments at**  
 227 **pH 9 and 10, and in the control. Error bars refer to the standard deviation among the 3 replicates.**

228



## 229 4 Discussion

230 Even if OAE using alkaline minerals is considered a promising tool to mitigate climate change through the sequestration  
231 and storage of atmospheric CO<sub>2</sub> into the ocean (DOSI, 2022), its impact on the marine ecosystem is still far to be  
232 understood. To the best of our knowledge, this is the first study investigating the potential effects of OAE on DOM  
233 dynamics, with particular regard to DOC concentration and CDOM optical properties. Given the crucial role that DOM  
234 plays in the marine ecosystem, any impact on its dynamics is expected to affect the water quality and ecosystem  
235 functioning through a cascading effect on the microbial loop and the microbial food web.

236

### 237 4.1 Liming impact on DOM dynamics

238 Our data show the potential effects of OAE on DOM dynamics determining a decrease in DOC concentration (Fig. 1 and  
239 4) and a change in the optical properties of CDOM (Fig. 2, 3, 5 and 6). The decrease in  $a_{254}$ , the increase in  $S_{275-295}$  (Fig.  
240 2 and 5) and the decrease in humic-like fluorescence (Fig. 3 and 6) indicate a change in DOM quality with a shift towards  
241 molecules with lower average molecular weight and aromaticity degree. These effects are already visible at pH 9, but  
242 becomes relevant at pH 10. Different hypotheses can explain our results:

- 243 1) DOM reacts with Ca(OH)<sub>2</sub> and the largest and most aromatic molecules are oxidized to CO<sub>2</sub>;
- 244 2) the largest and most aromatic molecules adsorb onto primary and secondary carbonate precipitates, that form  
245 following the Ca(OH)<sub>2</sub> addition, and sink;
- 246 3) the largest and most aromatic molecules aggregate forming polymer gels or large colloidal material and sink.

247 Interestingly, a significant decrease in DOC concentration was observed only in the unmixed samples at the end of the  
248 experiment (22 h after the addition, Fig. 1 and 4), DOC oxidation to CO<sub>2</sub> by reaction with Ca(OH)<sub>2</sub> (hypothesis 1) can  
249 therefore be ruled out as a possible removal mechanism. The other 2 hypotheses remain plausible and are supported by  
250 the available literature (Conzonno and Cirelli, 1995; Leenheer and Reddy, 2008; Pace et al., 2012).

251 In lake waters, DOM adsorbs onto carbonate particles and co-precipitates; the use of CaCO<sub>3</sub> precipitation was indeed  
252 suggested as an efficient technique for DOM removal during drinking water treatment processes (Leenheer and Reddy,  
253 2008). The mechanism of DOM co-precipitation and/or physical incorporation into CaCO<sub>3</sub> is due to the formation of  
254 insoluble calcium. This hypothesis is further supported by the observation of CaCO<sub>3</sub> precipitation following the  
255 dissolution of hydrated lime, that was enhanced by the occurrence of nucleation surfaces as particles or solid mineral  
256 phases in the solution (Moras et al., 2021).

257 In freshwater ponds, a high affinity of high molecular weight molecules to adsorb onto particles like CaCO<sub>3</sub> was observed  
258 by Conzonno and Cirelli (1995) together with a preferential removal of high molecular weight humic substances during  
259 CaCO<sub>3</sub> crystals formation. Since humic acids have important environmental functions in controlling the pH and the  
260 bioavailability of dissolved metals (Baalousha et al., 2006), their removal may trigger a cascade effect with possible  
261 impacts on water quality. Past studies showed that pH per se can affect DOM dynamics as DOM can undergo a fast  
262 transition from dissolved to polymer gels (Chin et al., 1998) or large colloidal material (Pace et al., 2012) when pH  
263 switches toward more basic values (pH > 8 for seawater).



264 Among the three hypotheses mentioned above, the observed decrease in  $a_{254}$ , observed in our experiments, supports the  
265 hypothesis 2, suggesting that, following the addition of  $\text{Ca}(\text{OH})_2$ , the largest and most aromatic dissolved organic  
266 molecules adsorb to primary and secondary mineral particles and sink.  
267

#### 268 **4.2 Different effects on Mediterranean and Baltic waters**

269 The MedSea and the BalSea are basins with different biogeochemical characteristics (Tab. 1). Our results show that DOC  
270 concentration (Fig. 1 and 4) and  $a_{254}$  (Fig. 2 and 5) are 6 and 13 times higher in the BalSea than in the MedSea (Tab. 1),  
271 these data are consistent with previous studies (Hoikkala et al., 2015; Santinelli et al., 2010; Santinelli, 2015). The lower  
272  $S_{275-295}$  (Tab. 1) and the different FDOM composition (Fig. S1 and S2) indicate a higher percentage of terrestrial DOM in  
273 the BalSea than in the Med Sea, as previously reported by Deutsch et al. (2012) and Hoikkala et al. (2015). Indeed, in the  
274 BalSea, PARAFAC allowed to characterize humic-like and fulvic-like components but not protein-like ones (Fig. S2,  
275 Tab. S3), differently from the MedSea where the protein-like component was identified (Fig. S1, Tab. S2). Protein-like  
276 compounds are usually related to in-situ production, whereas fulvic-like substances mostly have a terrestrial origin. The  
277 predominance of terrestrial DOM in the BalSea is due to the high freshwater input from the wide catchment area (~ 4  
278 times as large as the sea itself), and the low seawater input from the North Sea. The BalSea is also characterized by a  
279 peculiar carbonate system (Kuliński et al., 2017), exhibiting a wider range of total alkalinity (and pH) compared to the  
280 oceans. In particular, the Gulf of Riga, where the water for our experiment was collected, is characterized by a higher  
281 total alkalinity and a higher pH with respect to the rest of the BalSea (Beldowski et al., 2010; Kuliński et al., 2017).

282 In our experiment, we observed a different impact of  $\text{Ca}(\text{OH})_2$  addition in the MedSea and BalSea water. In the MedSea,  
283 a DOC decrease of 8 and 11  $\mu\text{M}$  was recorded at pH 9 and 10, respectively, indicating a net removal up to 16% of the  
284 initial DOC (Fig. 1). In the BalSea, the maximum removal observed was 8% at pH 10, whereas no effect was recorded at  
285 pH 9 (Fig. 4).

286 Even if the salinity, being markedly lower in the BalSea than in the MedSea, is probably the main driver of the lower  
287 precipitation of  $\text{CaCO}_3$ , and consequently of the less pronounced effects on DOM dynamic, it cannot be excluded that the  
288 peculiar carbonate system combined with the different concentration and quality of DOM may have influenced the lower  
289 removal rates observed in our experiment. The influence of water chemistry is already evident by the 4-times lower  
290 amount of  $\text{Ca}(\text{OH})_2$  needed to reach pH 9 and 10 in the BalSea than in the MedSea. Since  $\text{CaCO}_3$  precipitation can be  
291 one of the main mechanisms explaining our results, the lower amount of  $\text{Ca}(\text{OH})_2$  added in the BalSea can explain the  
292 lower decrease of DOC observed in this basin than in the MedSea.

293 It is noteworthy that DOM in the MedSea and in the oceans shows a clear seasonal cycle, mostly attributed to the changes  
294 in temperature, water stratification and biological activity, affecting DOM concentration, optical properties and  
295 stoichiometry (Carlson and Hansell, 2015; Santinelli et al., 2013; Santinelli, 2015). Seasonality strongly affects DOM  
296 dynamics also in the BalSea with prevalent allochthonous sources in winter and in-situ production by phytoplankton in  
297 spring (Seidel et al., 2017; Hoikkala et al., 2012). By integrating these observations with the outcomes of our study, it  
298 becomes evident that any hypothesis of liming-based OAE should not only account for the physico-chemical properties  
299 of each basin but also consider seasonal variability.

300



301 **4.3 Changed DOM dynamics: implication for the marine ecosystems**

302 Our results suggest that  $\text{CaCO}_3$  precipitation is the main driver for the sequestration of DOM from the water column. The  
303 sinking of the largest and most complex fraction of DOM to the deep oceans could lead to different scenarios.

304 1. If the exported DOC is labile (i.e. it is available to microbial removal on the short temporal scale), its export would  
305 determine:

306 • A depletion of the energy available for heterotrophic prokaryotes in the surface layer, determining a  
307 malfunctioning of the microbial loop that could impact the energy transfer to the higher trophic levels. This  
308 process could be further enhanced if the primary production is limited by the reduced water transparency  
309 due to carbonate formation.

310 • The export of energy to the deepest layer (below the carbon compensation depth, CCD), leading to an  
311 increased bacterial production, in response to the labile DOM released due to the  $\text{CaCO}_3$  dissolution.

312 2. If the exported DOC is refractory (i.e. it is not available to microbial removal on the short temporal scale), it will  
313 contribute to C sequestration in the deep waters.

314

315 **5. Conclusions**

316 This study reports the first evidence of the potential effects of OAE on DOM dynamics in two contrasting environments:  
317 the oligotrophic MedSea, known for its low DOC concentration, and the eutrophic BalSea, characterized by high DOM  
318 concentration mostly of terrestrial origin. Our findings suggest that ocean alkalization by  $\text{Ca}(\text{OH})_2$  sparging may alter  
319 DOM dynamics and, consequently, have a potential impact on the entire marine ecosystem. To mitigate these effects, it  
320 is crucial to reduce the duration and intensity of pH spikes, ensuring they remain below the safety threshold of pH 9. We  
321 stress the need to take into consideration the physico-chemical properties (e.g. salinity, pH, DOM concentration and  
322 quality) of the basin and the season, to efficiently manage ocean liming and mitigate the potential impacts of ocean  
323 alkalization on DOM pool.

324 Although the experimental conditions used in this study were more severe than actual liming practices, where the release  
325 of  $\text{Ca}(\text{OH})_2$  in the ship's wake undergoes rapid dilution that significantly reduces pH changes, our results provide new  
326 insights into the possible impacts due to physico-chemical processes.

327 It is important to highlight that the experiments in this study were conducted using sterilized seawater, thus excluding the  
328 potential interplay of biological processes on DOM dynamics. To gain a more comprehensive understanding of possible  
329 OAE impacts, future research should address the influence of biological processes, as well as factors like dilution rates,  
330 water mixing, and realistic durations and severities of pH peaks. Scaling up the experimental setup to mesocosms would  
331 allow for repeated additions and longer observation periods, enabling a more accurate representation of real-world  
332 conditions.

333

334 **Author contribution**



335 Conceptualization by CS, DB and AA. CS designed and supervised the experiments and SV, RBS, GB, GC, MG carried them out.

336 Funding acquisition by SC and AA. CS prepared the manuscript with contributions from all co-authors.

337

### 338 **Competing interests**

339 The authors declare that they have no conflict of interest.

340

### 341 **Acknowledgements**

342 The current study has received funding from European Lime Association (EuLA) through a research contract established with CoNISMa  
343 (National Inter-University Consortium for Marine Sciences) in Italy. We warmly thank Roberto Moreschi and Dario Ravasio  
344 (UNICALCE Sedrina) for kindly sending the samples of Ca-hydroxide used for our experiments. We thank Giovanni Cappello  
345 (Limenet) and Agija Bistere (Hyrogas) for sampling and sending to Pisa the Baltic seawater. The authors are grateful to Marco Carloni  
346 and Valtere Evangelista for their support in sampling of MedSea water and CDOM/FDOM analyses and to Rosanna Cascone, Rosanna  
347 Claps and Claudia Neri, (IBF-CNR, Italy) for the assistance in the financial management. The authors wish to thank Aurela Shitza and  
348 Marlena Wissel from EuLA for their valuable feedback and helpful suggestions which greatly contributed to the overall improvement  
349 of this paper.

350



351 **References**

- 352 Baalousha, M., Kammer, F. V. D., Motelica-Heino, M., Hilal, H. S., and Le Coustumer, P.: Size fractionation and  
353 characterization of natural colloids by flow-field flow fractionation coupled to multi-angle laser light scattering, *J*  
354 *Chromatogr A*, 1104, 272–281, <https://doi.org/10.1016/j.chroma.2005.11.095>, 2006.
- 355 Beldowski, J., Löffler, A., Schneider, B., and Joensuu, L.: Distribution and biogeochemical control of total CO<sub>2</sub> and  
356 total alkalinity in the Baltic Sea, *Journal of Marine Systems*, 81, 252–259,  
357 <https://doi.org/10.1016/j.jmarsys.2009.12.020>, 2010.
- 358 Butenschön, M., Lovato, T., Masina, S., Caserini, S., and Grosso, M.: Alkalinization Scenarios in the Mediterranean  
359 Sea for Efficient Removal of Atmospheric CO<sub>2</sub> and the Mitigation of Ocean Acidification, *Frontiers in Climate*, 3,  
360 614537, <https://doi.org/10.3389/fclim.2021.614537>, 2021.
- 361 Calvin, K., Dasgupta, D., Krinner, G., Mukherji, A., Thorne, P. W., Trisos, C., Romero, J., Aldunce, P., Barrett, K.,  
362 Blanco, G., Cheung, W. W. L., Connors, S., Denton, F., Diongue-Niang, A., Dodman, D., Garschagen, M., Geden, O.,  
363 Hayward, B., Jones, C., Jotzo, F., Krug, T., Lasco, R., Lee, Y.-Y., Masson-Delmotte, V., Meinshausen, M.,  
364 Mintenbeck, K., Mokssit, A., Otto, F. E. L., Pathak, M., Pirani, A., Poloczanska, E., Pörtner, H.-O., Revi, A., Roberts,  
365 D. C., Roy, J., Ruane, A. C., Skea, J., Shukla, P. R., Slade, R., Slangen, A., Sokona, Y., Sörensson, A. A., Tignor, M.,  
366 van Vuuren, D., Wei, Y.-M., Winkler, H., Zhai, P., Zommers, Z., Hourcade, J.-C., Johnson, F. X., Pachauri, S.,  
367 Simpson, N. P., Singh, C., Thomas, A., Totin, E., Alegría, A., Armour, K., Bednar-Friedl, B., Blok, K., Cissé, G.,  
368 Dentener, F., Eriksen, S., Fischer, E., Garner, G., Guivarch, C., Haasnoot, M., Hansen, G., Hauser, M., Hawkins, E.,  
369 Hermans, T., Kopp, R., Leprince-Ringuet, N., Lewis, J., Ley, D., Ludden, C., Niamir, L., Nicholls, Z., Some, S., Szopa,  
370 S., Trewin, B., van der Wijst, K.-I., Winter, G., Witting, M., Birt, A., and Ha, M.: IPCC, 2023: Climate Change 2023:  
371 Synthesis Report. Contribution of Working Groups I, II and III to the Sixth Assessment Report of the Intergovernmental  
372 Panel on Climate Change [Core Writing Team, H. Lee and J. Romero (eds.)]. IPCC, Geneva, Switzerland.,  
373 <https://doi.org/10.59327/IPCC/AR6-9789291691647>, 2023.
- 374 Camatti, E., Valsecchi, S., Caserini, S., Barbaccia, E., Santinelli, C., Basso, D., and Azzellino, A.: Short-term impact  
375 assessment of ocean liming: A copepod exposure test, *Mar Pollut Bull*, 198, 115833,  
376 <https://doi.org/10.1016/j.marpolbul.2023.115833>, 2024.
- 377 Carlson, C. A. and Hansell, D. A.: DOM Sources, Sinks, Reactivity, and Budgets, in: *Biogeochemistry of Marine*  
378 *Dissolved Organic Matter*, 65–126, <https://doi.org/10.1016/B978-0-12-405940-5.00003-0>, 2015.
- 379 Caserini, S., Pagano, D., Campo, F., Abbà, A., De Marco, S., Righi, D., Renforth, P., and Grosso, M.: Potential of  
380 Maritime Transport for Ocean Liming and Atmospheric CO<sub>2</sub> Removal, *Frontiers in Climate*, 3, 575900,  
381 <https://doi.org/10.3389/fclim.2021.575900>, 2021.
- 382 Chikamoto, M. O., DiNezio, P., and Lovenduski, N.: Long-Term Slowdown of Ocean Carbon Uptake by Alkalinity  
383 Dynamics, *Geophys Res Lett*, 50, <https://doi.org/10.1029/2022GL101954>, 2023.
- 384 Chin, W.-C., Orellana, M. V., and Verdugo, P.: Spontaneous assembly of marine dissolved organic matter into polymer  
385 gels, *Nature*, 391, 568–572, <https://doi.org/10.1038/35345>, 1998.
- 386 Coble, P.: Characterization of marine and terrestrial DOM in seawater using excitation-emission matrix spectroscopy,  
387 *Mar Chem*, 51, 325–346, 1996.
- 388 Conzonno, V. H. and Cirelli, A. F.: Dissolved organic matter in Chascomus Pond (Argentina). Influence of calcium  
389 carbonate on humic acid concentration, *Hydrobiologia*, 297, 55–59, <https://doi.org/10.1007/BF00033501>, 1995.
- 390 Deutsch, B., Alling, V., Humborg, C., Korth, F., and Mörth, C. M.: Tracing inputs of terrestrial high molecular weight  
391 dissolved organic matter within the Baltic Sea ecosystem, *Biogeosciences*, 9, 4465–4475, <https://doi.org/10.5194/bg-9-4465-2012>, 2012.
- 393 DOSI: Ocean Alkalinity Enhancement Deep Ocean Stewardship Initiative Policy Brief, 2022.
- 394 Gattuso, J.-P., Mach, K. J., and Morgan, G.: Ocean acidification and its impacts: an expert survey, *Clim Change*, 117,  
395 725–738, <https://doi.org/10.1007/s10584-012-0591-5>, 2013.
- 396 González, M. F. and Ilyina, T.: Impacts of artificial ocean alkalinization on the carbon cycle and climate in Earth  
397 system simulations, *Geophys Res Lett*, 43, 6493–6502, <https://doi.org/10.1002/2016GL068576>, 2016.





- 398 Gore, S., Renforth, P., and Perkins, R.: The potential environmental response to increasing ocean alkalinity for negative  
399 emissions, *Mitig Adapt Strateg Glob Chang*, 24, 1191–1211, <https://doi.org/10.1007/s11027-018-9830-z>, 2019.
- 400 Hansell, D., Carlson, C., Repeta, D., and Schlitzer, R.: Dissolved Organic Matter in the Ocean: A Controversy  
401 Stimulates New Insights, *Oceanography*, 22, 202–211, <https://doi.org/10.5670/oceanog.2009.109>, 2009.
- 402 Hansell, D. A.: Dissolved Organic Carbon Reference Material Program, *Eos, Transactions American Geophysical  
403 Union*, 86, 318, <https://doi.org/10.1029/2005EO350003>, 2005.
- 404 Heinze, C., Meyer, S., Goris, N., Anderson, L., Steinfeldt, R., Chang, N., Le Quéré, C., and Bakker, D. C. E.: The ocean  
405 carbon sink – impacts, vulnerabilities and challenges, *Earth System Dynamics*, 6, 327–358, <https://doi.org/10.5194/esd-6-327-2015>, 2015.
- 407 Helms, J. R., Stubbins, A., Ritchie, J. D., Minor, E. C., Kieber, D. J., and Mopper, K.: Absorption spectral slopes and  
408 slope ratios as indicators of molecular weight, source, and photobleaching of chromophoric dissolved organic matter,  
409 *Limnol Oceanogr*, 53, 955–969, <https://doi.org/10.4319/lo.2008.53.3.0955>, 2008.
- 410 Hoikkala, L., Lahtinen, T., Perttilä, M., and Lignell, R.: Seasonal dynamics of dissolved organic matter on a coastal  
411 salinity gradient in the northern Baltic Sea, *Cont Shelf Res*, 45, 1–14, <https://doi.org/10.1016/j.csr.2012.04.008>, 2012.
- 412 Hoikkala, L., Kortelainen, P., Soinne, H., and Kuosa, H.: Dissolved organic matter in the Baltic Sea, *Journal of Marine  
413 Systems*, 142, 47–61, <https://doi.org/10.1016/j.jmarsys.2014.10.005>, 2015.
- 414 Khesghi, H. S.: Sequestering atmospheric carbon dioxide by increasing ocean alkalinity, *Energy*, 20, 915–922,  
415 [https://doi.org/10.1016/0360-5442\(95\)00035-F](https://doi.org/10.1016/0360-5442(95)00035-F), 1995.
- 416 Kuliński, K., Schneider, B., Szymczycha, B., and Stokowski, M.: Structure and functioning of the acid–base system in  
417 the Baltic Sea, *Earth System Dynamics*, 8, 1107–1120, <https://doi.org/10.5194/esd-8-1107-2017>, 2017.
- 418 Lawaetz, A. J. and Stedmon, C. A.: Fluorescence intensity calibration using the Raman scatter peak of water, *Appl  
419 Spectrosc*, 63, 936–940, <https://doi.org/10.1366/000370209788964548>, 2009.
- 420 Leenheer, J. A. and Reddy, M. M.: CO-PRECIPIATION OF DISSOLVED ORGANIC MATTER BY CALCIUM  
421 CARBONATE IN PYRAMID LAKE, NEVADA, *Annals of Environmental Science*, 2008.
- 422 Moras, P., Mentş, T. O., Schiller, F., Ferrari, L., Topwal, D., Locatelli, A., Sheverdyeva, P. M., and Carbone, C.:  
423 Reference plane for the electronic states in thin films on stepped surfaces, *Phys Rev B*, 103, 165426,  
424 <https://doi.org/10.1103/PhysRevB.103.165426>, 2021.
- 425 Murphy, K. R., Stedmon, C. A., Graeber, D., and Bro, R.: Fluorescence spectroscopy and multi-way techniques.  
426 PARAFAC, *Analytical Methods*, 5, 6557, <https://doi.org/10.1039/c3ay41160e>, 2013.
- 427 Murphy, K. R., Stedmon, C. A., Wenig, P., and Bro, R.: OpenFluor- an online spectral library of auto-fluorescence by  
428 organic compounds in the environment, *Analytical Methods*, 6, 658–661, <https://doi.org/10.1039/C3AY41935E>, 2014.
- 429 Omanović, D., Santinelli, C., Marcinek, S., and Gonnelli, M.: ASFit - An all-inclusive tool for analysis of UV–Vis  
430 spectra of colored dissolved organic matter (CDOM), *Comput Geosci*, 133, 104334,  
431 <https://doi.org/10.1016/j.cageo.2019.104334>, 2019.
- 432 Omanović, D., Marcinek, S., and Santinelli, C.: TreatEEM—A Software Tool for the Interpretation of Fluorescence  
433 Excitation-Emission Matrices (EEMs) of Dissolved Organic Matter in Natural Waters, *Water (Basel)*, 15, 2214,  
434 <https://doi.org/10.3390/w15122214>, 2023.
- 435 Pace, M. L., Reche, I., Cole, J. J., Fernández-Barbero, A., Mazuecos, I. P., and Prairie, Y. T.: pH change induces shifts  
436 in the size and light absorption of dissolved organic matter, *Biogeochemistry*, 108, 109–118,  
437 <https://doi.org/10.1007/s10533-011-9576-0>, 2012.
- 438 Royal Society and Royal Academy of Engineering: Greenhouse Gas Removal, 2018.
- 439 Santinelli, C.: DOC in the Mediterranean Sea, in: *Biogeochemistry of Marine Dissolved Organic Matter*, edited by:  
440 Hansell, D. A., Elsevier, 579–608, <https://doi.org/10.1016/B978-0-12-405940-5.00013-3>, 2015.





- 441 Santinelli, C., Nannicini, L., and Seritti, A.: DOC dynamics in the meso and bathypelagic layers of the Mediterranean  
442 Sea, *Deep Sea Research Part II: Topical Studies in Oceanography*, 57, 1446–1459,  
443 <https://doi.org/10.1016/j.dsr2.2010.02.014>, 2010.
- 444 Santinelli, C., Hansell, D. A., and Ribera d'Alcalà, M.: Influence of stratification on marine dissolved organic carbon  
445 (DOC) dynamics: The Mediterranean Sea case, *Prog Oceanogr*, 119, 68–77,  
446 <https://doi.org/10.1016/j.pocean.2013.06.001>, 2013.
- 447 Santinelli, C., Follett, C., Retelletti Brogi, S., Xu, L., and Repeta, D.: Carbon isotope measurements reveal unexpected  
448 cycling of dissolved organic matter in the deep Mediterranean Sea, *Mar Chem*, 177, 267–277,  
449 <https://doi.org/10.1016/j.marchem.2015.06.018>, 2015.
- 450 Seidel, M., Manecki, M., Herlemann, D. P. R., Deutsch, B., Schulz-Bull, D., Jürgens, K., and Dittmar, T.: Composition  
451 and Transformation of Dissolved Organic Matter in the Baltic Sea, *Front Earth Sci (Lausanne)*, 5,  
452 <https://doi.org/10.3389/feart.2017.00031>, 2017.
- 453 Del Vecchio, R. and Blough, N. V.: Spatial and seasonal distribution of chromophoric dissolved organic matter and  
454 dissolved organic carbon in the Middle Atlantic Bight, in: *Marine Chemistry*, 169–187,  
455 <https://doi.org/10.1016/j.marchem.2004.02.027>, 2004.
- 456 Weishaar, J., Aiken, G., Bergamaschi, B., Fram, M., Fujii, R., and Mopper, K.: Evaluation of specific ultra-violet  
457 absorbance as an indicator of the chemical content of dissolved organic carbon, *Environ Sci Technol*, 37, 4702–4708,  
458 <https://doi.org/10.1021/es030360x>, 2003.
- 459